

# JOURNAL OF THE GEOTECHNICAL ENGINEERING DIVISION

## DEFORMATION AND STRENGTH CHARACTERISTICS OF SOFT BANGKOK CLAY

By A. S. Balasubramaniam,<sup>1</sup> M. ASCE and A. R. Chaudhry<sup>2</sup>

### INTRODUCTION

Several stress-strain theories have recently been developed to describe the stress-strain behavior of normally consolidated clays; Roscoe and Poorooshasb (14); Roscoe, Schofield, and Thurairajah (15); Roscoe and Burland (13), and Schofield and Wroth (17). The predictions from these theories are often compared with the observations on specimens of Kaolin prepared in the laboratory and tested under controlled conditions (3–6,8).

As a logical extension of the extensive work (1–5,8) carried out on specimens of Kaolin prepared under controlled conditions in the laboratory, the present paper deals with a detailed study of the deformation characteristics of undisturbed specimens of soft Bangkok clay. The experimental observations from a large number of tests conducted with different applied stress paths are compared with the predictions made by the various stress-strain theories developed at Cambridge. This study is an initial phase of the application of recent theories to the solution of boundary value problems in practice, i.e., embankments and excavations on soft clay deposits.

### BASIC CONCEPTS AND DEFINITIONS

The stress parameters  $p'$  and  $q$  are defined by

$$p' = \frac{\sigma'_1 + 2\sigma'_3}{3} \dots\dots\dots (1a)$$

$$\text{and } q = \sigma'_1 - \sigma'_3 \dots\dots\dots (1b)$$

Note.—Discussion open until February 1, 1979. To extend the closing date one month, a written request must be filed with the Editor of Technical Publications, ASCE. This paper is part of the copyrighted Journal of the Geotechnical Engineering Division, Proceedings of the American Society of Civil Engineers, Vol. 104, No. GT9, September, 1978. Manuscript was submitted for review for possible publication on November 1, 1977.

<sup>1</sup>Assoc. Prof. in Geotechnical Engrg., Asian Inst. of Tech., Bangkok, Thailand.

<sup>2</sup>Lect. in Civ. Engrg., Univ. of Basrah, Basrah, Iraq.

in which  $\sigma'_1$ ,  $\sigma'_2$ , and  $\sigma'_3$  are the principal effective compressive stresses;  $\sigma'_2 = \sigma'_3$  under the triaxial stress system; and  $p'$  and  $q$  are referred to as the mean normal stress and deviator stress, respectively. The stress ratio,  $q/p'$ , is denoted by  $\eta$ . The stress parameter,  $p_e$ , is called the mean equivalent pressure and is defined as

$$p_e = p'_o \exp \left( \frac{e_o - e}{\lambda} \right) \dots \dots \dots (2)$$

in which  $p'_o$  and  $e_o$  correspond to the preshear consolidation pressure and voids ratio on the isotropic consolidation line; and  $\lambda$  is the slope of the isotropic consolidation line in the  $e$ ,  $\log p'$  plot. During undrained tests, there is no change in voids ratio and, therefore,  $p_e$  remains constant during shear at a value of  $p'_o$ . However, during a drained test in which the voids ratio,  $e$ , decreases, the mean equivalent pressure,  $p_e$ , increases from its initial value of  $p'_o$ .

The incremental strain parameters  $dv$  and  $d\epsilon$  are

$$dv = d\epsilon_1 + 2d\epsilon_3 \dots \dots \dots (3a)$$

$$\text{and } d\epsilon = \frac{2(d\epsilon_1 - d\epsilon_3)}{3} \dots \dots \dots (3b)$$

in which  $d\epsilon_1$ ,  $d\epsilon_2$ , and  $d\epsilon_3$  are the principal incremental compressive strains; and  $d\epsilon_2 = d\epsilon_3$  under the triaxial stress system. The axial and volumetric strains are defined as

$$\epsilon_1 = \log \frac{l_o}{l} \dots \dots \dots (4a)$$

$$\text{and } v = \log \frac{V_o}{V} \dots \dots \dots (4b)$$

in which  $l_o$  and  $V_o$  are the initial height and volume of the sample;  $l$  and  $V$  correspond to current values; and  $\epsilon_1$  and  $v$  correspond to natural strains. If the corresponding cumulative strains (as usually adapted by geotechnical engineers) are  $\epsilon_1^*$  and  $v^*$ , then

$$\epsilon_1 = \epsilon_1^* + \frac{1}{2} (\epsilon_1^*)^2 + \frac{1}{3} (\epsilon_1^*)^3 + \dots \dots \dots (5a)$$

$$\text{and } v = v^* + \frac{1}{2} (v^*)^2 + \frac{1}{3} (v^*)^3 + \dots \dots \dots (5b)$$

For all purposes, the terms higher than the third order may be neglected. Also, at low levels of strains both the natural strains and cumulative strains are very nearly the same. However, at large strains deviations do occur and it is customary to use natural strains in the study of plastically deforming materials (13-17).

#### MATERIAL TESTED, SAMPLE PREPARATION, AND TESTING PROCEDURE

A detailed description of the general properties of soft Bangkok clay is given by the first writer, et al. (6). The maximum past pressure of the clay is 69

$\text{kN/m}^2$ . The undisturbed samples were taken at a depth of 5.5 m–6 m. The average index properties and natural water content are as follows: (1) Natural water content = 112%–130%; (2) liquid limit =  $118.0\% \pm 2\%$ ; (3) plastic limit =  $43.0 \pm 2\%$ ; and (4) plasticity index =  $75\% \pm 4\%$ . The triaxial specimens were 36 mm in diameter and 77 mm in height. All tests were carried out under stress controlled conditions, and a back pressure of  $207 \text{ kN/m}^2$  was used to saturate the specimens.

## RESULTS OF UNDRAINED TESTS

The test series I and II included undrained tests with 1-hr and 1-day load increment durations. Altogether, 12 specimens were sheared in these tests. The behavior of the specimens sheared under 1-hr load increment duration and 1-day load increment duration were virtually the same. Therefore, the results of the specimens sheared under 1-hr load increment duration only will be presented here. In this series, five undrained tests were carried out on specimens isotropically consolidated to stresses of  $138 \text{ kN/m}^2$ ,  $207 \text{ kN/m}^2$ ,  $276 \text{ kN/m}^2$ ,  $345 \text{ kN/m}^2$ , and  $414 \text{ kN/m}^2$ . These specimens were subsequently sheared with increasing axial stress and under constant cell pressure.

**Effective Stress Paths.**—Fig. 1 shows the effective stress paths followed by the specimens in the  $q, p'$  plot. The dashed lines in this figure correspond to constant shear strain contours and will be considered in the subsequent section. The effective stress paths are found to be virtually similar. Each effective stress path corresponds to a constant water content contour (7,12). Since the effective stress paths are similar, it is possible to normalize them by using the parameters  $q/p_e$  and  $p'/p_e$ , where, in an undrained test,  $p_e$  corresponds to the preshear consolidation pressure. Fig. 2 shows the state paths followed by all the test specimens in a  $q/p_e, p'/p_e$  plot. The state paths followed by the specimens are found to be approximately the same.

**Shear Strain Contours.**—The deviator stress-shear strain relationships for all specimens are shown in Fig. 3(a). Constant shear strain contours are superimposed on the effective stress paths in Fig. 1. It is noted that the constant shear strain contours are linear and pass through the origin. A similar finding was reported for Weald clay and London clay by Roscoe and Poorooshasb (14) and for Kaolin by Roscoe, Schofield, and Thurairajah (15) and the first writer (2). Ladd (9) and Lamb (10) have also shown similar plots but with an alternate set of definitions for stress parameters. This implies that, for all specimens of soft Bangkok clay sheared under undrained conditions, the  $q/p', \epsilon$  relationship is independent of the preshear consolidation pressure. Fig. 3(b) shows the variation of shear strain,  $\epsilon$ , and the stress ratio  $q/p'$ . The relationship can be expressed as

$$\epsilon = \int_0^{\eta} f_1(\eta) d\eta \quad \dots \dots \dots (6a)$$

Thus the incremental strain,  $d\epsilon$ , corresponding to any increment in stress can be expressed as

$$d\epsilon = f_1(\eta) d\eta \quad \dots \dots \dots (6b)$$

The shear strain,  $\epsilon$ , during an undrained test is thus only dependent on the magnitude of the stress ratio,  $\eta$  (13–16).

**Pore Pressure-Shear Strain Relationship.**—The pore pressure-shear strain relationships of the specimens are shown in Fig. 3(c). The  $u, \epsilon$  relationships are similar. The corresponding variation of the pore pressure parameter,  $A$  (18),

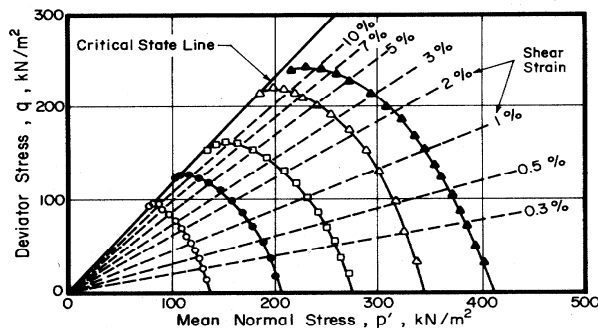


**FIG. 1.—Effective Stress Paths Followed by Specimens in Undrained Tests with Constant Cell Pressure**

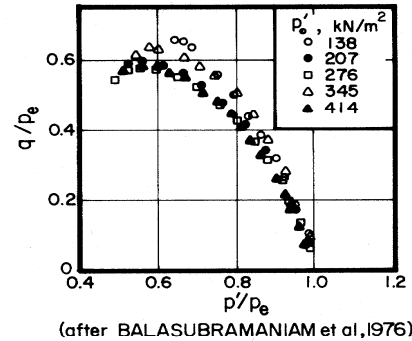


**FIG. 2.—State Paths Followed by Undrained Test Specimens**

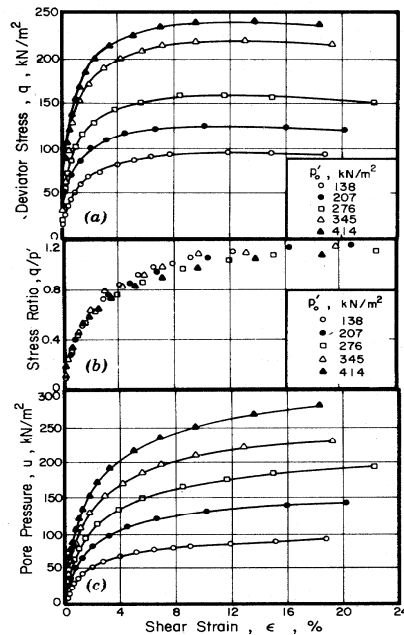


**FIG. 3.—Undrained Test Specimens: (a)  $q, \epsilon$  Specimen; (b)  $q/p', \epsilon$  Relationship**

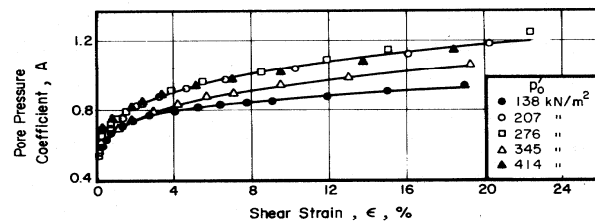


**FIG. 4.— $A, \epsilon$  Relationship**

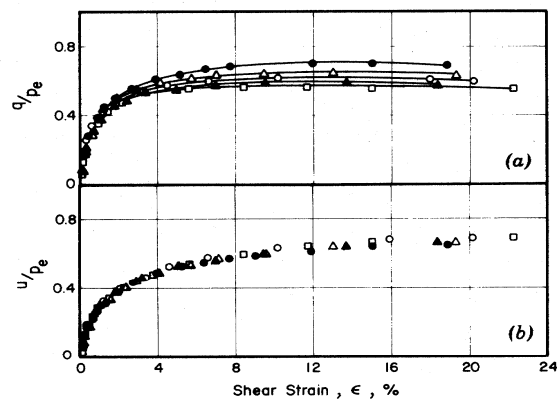


**FIG. 5.—Undrained Tests: (a) Normalized Deviator Stress-Shear Strain Relationship; (b) Normalized Pore Pressure-Shear Strain Relationship**

with strain is shown in Fig. 4. The  $A$  parameter starts with a value of about 0.55 and increases rapidly with strain up to about 2% and, thereafter, the rate of increase is small. The tests conducted at 207-kN/m<sup>2</sup>, 276-kN/m<sup>2</sup>, and

414-kN/m<sup>2</sup> consolidation pressures do have an identical  $A$ ,  $\epsilon$  relationship. However, the specimens sheared from 138-kN/m<sup>2</sup> and 207-kN/m<sup>2</sup> consolidation pressures failed at a lower value of  $A$  as compared to the other samples.

**Normalized Stress-Strain Behavior.**—The deviator stress-shear strain relationship and the pore-water pressure-shear strain relationships are normalized by dividing the stresses with the preshear consolidation pressure. Fig. 5(a) shows the variation of the normalized deviator stress with shear strain. The normalized behavior is found to be the same and is not dependent on the preshear consolidation

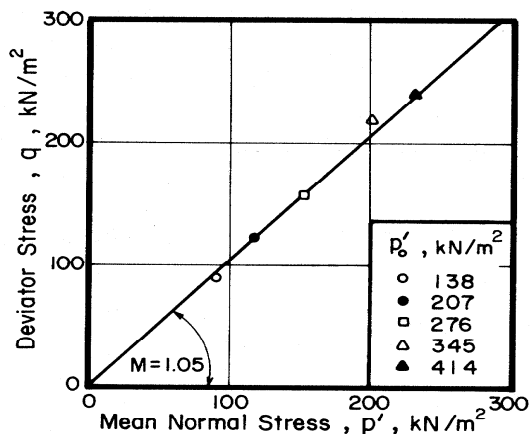


FIG. 6.—Peak Stress Points for Specimens Sheared in Undrained Tests

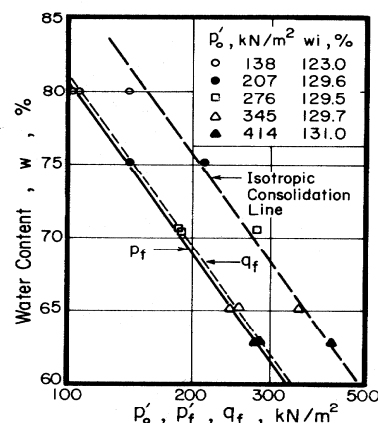


FIG. 7.—States of Samples at Failure in  $w$ ,  $\log p'$  and  $w$ ,  $\log q$  Plots

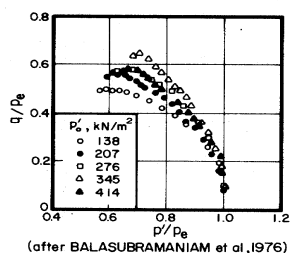


FIG. 8.—State Paths Followed during Fully Drained Tests with Constant Cell Pressure

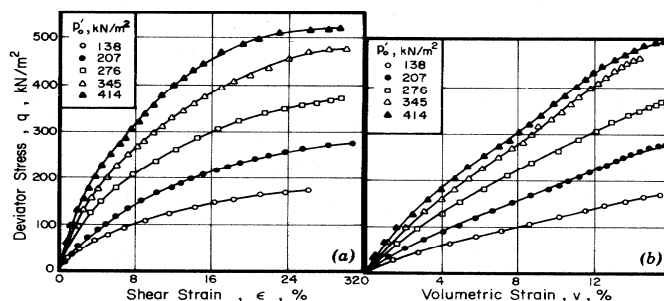


FIG. 9.—Fully Drained Tests with Constant Cell Pressure: (a)  $q$ ,  $\epsilon$  Relationship; (b)  $q$ ,  $v$  Relationship

pressure. Such a normalized behavior was originally noted by Ladd (9). The normalized pore pressure-strain relationships are presented in Fig. 5(b). At failure, the normalized pore pressures in all the specimens reached almost a constant value.

**Peak Stress Conditions.**—The values of the peak stresses are plotted in Fig. 6 in the  $q$ ,  $p'$  plot. The end points or the failure points are found to lie on a straight line that passes through the origin. The slope,  $M$ , of this line is found to be 1.05, the corresponding value of  $\bar{\phi}$  being 26°. The end points of the specimens at failure are plotted in Fig. 7 in the  $w$ ,  $\log p'$  plot. In this

plot, the water content at failure is found to vary linearly with the logarithm of the mean normal stress and the deviator stress. Also, the variation is found

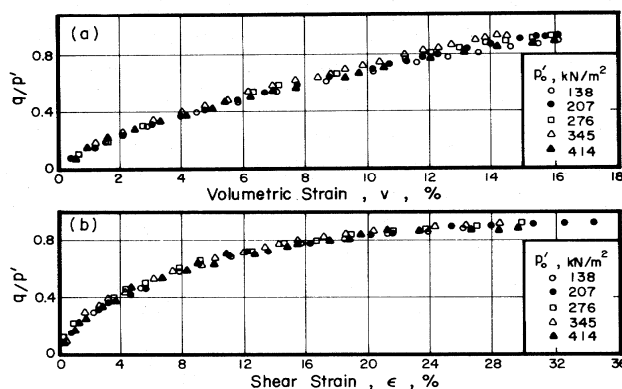


FIG. 10.—Fully Drained Tests with Constant Cell Pressure: (a)  $q/p'$ ,  $\epsilon$  Relationship; (b)  $q/p'$ ,  $v$  Relationship

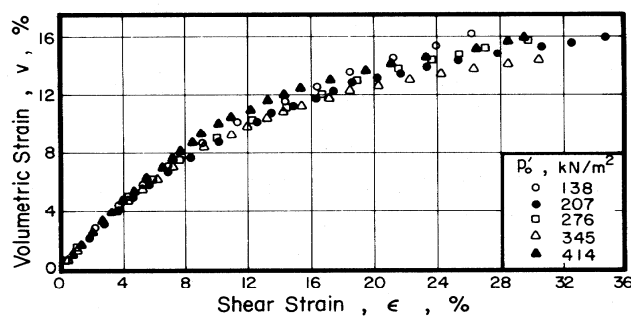


FIG. 11.— $v$ ,  $\epsilon$  Relationship for Fully Drained Tests with Constant Cell Pressure

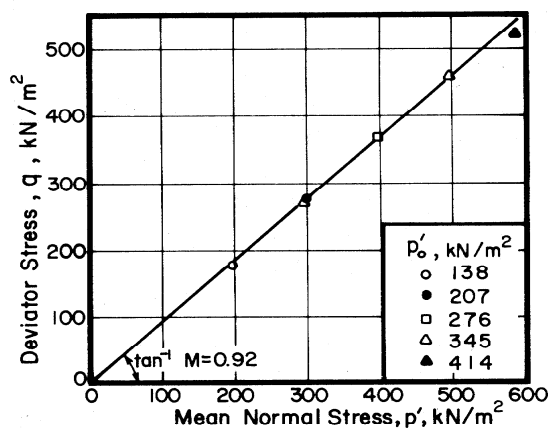


FIG. 12.—Peak Stress Points for Drained Test Specimens in  $q$ ,  $p'$  Plot

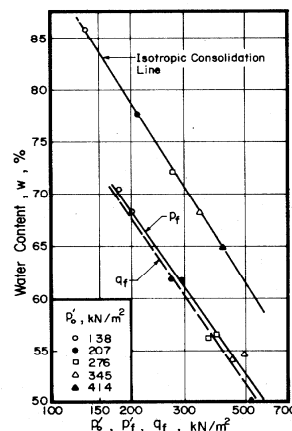


FIG. 13.—States of Samples at Failure in  $w$ ,  $\log p'$  Plot

to be nearly parallel to the corresponding variation during isotropic consolidation.

A comparison of the test data made from tests with 1-hr load increment

duration and 1-day load increment duration have indicated that almost all the behavior reviewed previously is virtually the same in both types of tests. It thus appears that, in a continuous stress controlled undrained test, the load increment durations have very little effect on the stress-strain behavior and strength characteristics. Similar findings were reported by Walker (19) and the first writer (1) for remolded specimens of Kaolin.

#### RESULTS OF FULLY DRAINED TESTS WITH CONSTANT CELL PRESSURE

In this series of tests, five fully drained tests were carried out on soft Nong Ngoo Hao clay, isotropically consolidated to preshear consolidation pressures of 138 kN/m<sup>2</sup>, 207 kN/m<sup>2</sup>, 275 kN/m<sup>2</sup>, 345 kN/m<sup>2</sup>, and 414 kN/m<sup>2</sup>. All specimens were sheared under stress controlled conditions. The procedure adopted for the selection of load increment size and duration was similar to that adopted by the first writer (2). The cell pressure was maintained constant and the axial stress was increased. The applied stress paths will be linear in the  $q, p'$  plot with  $dq/dp' = 3$ .

**State Paths.**—The state paths followed by the specimens are shown in Fig. 8. The state paths corresponding to isotropic stresses of 207 kN/m<sup>2</sup>, 276 kN/m<sup>2</sup>, and 414 kN/m<sup>2</sup> are found to be nearly the same. The slight deviations exhibited by the other samples are covered in an earlier publication (6).

**Stress-Strain Relationship.**—Fig. 9 shows the  $q, \epsilon$  and  $q, \nu$  relationships. Well-defined peak was not observed in any of the stress-strain curves. In both plots, the deviator stress corresponding to any level of strain is found to be more or less proportional to the preshear consolidation pressure.

**Stress Ratio Strain Relationship.**—For normally consolidated clays for any one type of applied stress path, unique stress ratio strain relationship was reported by Roscoe and Poorooshasb (14), Wroth (20), Mitchell (11), and the first writer (2). It would thus be interesting to study the  $q/p', \nu$  and  $q/p', \epsilon$  relationships for soft Bangkok clay. These relationships are shown in Figs. 10(a) and 10(b). Both the volumetric strain and the shear strain are found to vary in a unique manner with respect to the stress ratio.

**Volumetric Strain-Shear Strain Relationship.**—The  $\nu, \epsilon$  relationships for all the specimens sheared from the different preshear consolidation pressure are shown in Fig. 11. The  $\nu, \epsilon$  relationship is unique. Also at large strain, volumetric strain virtually reaches a steady value.

**Peak Stress Conditions.**—The end points of the specimens are shown in Figs. 12 and 13 in the  $q, p', w, \log p'$ , and  $w, \log q$  plots. These results are in agreement with the critical state concept of Roscoe, Schofield and Wroth (16). The slope,  $M$ , of the critical state line in the  $q, p'$  plot is 0.92. This corresponds to an angle of internal friction  $\bar{\phi}$  of 21.7°. Furthermore, the projections of the critical state line in the  $w, \log p'$  and  $w, \log q$  plots are found to be parallel to the isotropic consolidation line. The value of  $M$  obtained for drained tests is lower than that for undrained tests. This deviation will be examined subsequently, after presenting the test results for constant  $p'$  tests.

#### RESULTS OF CONSTANT $p'$ DRAINED TESTS

In this series of tests four specimens were sheared under constant  $p'$  drained conditions from preshear consolidation pressures of 138 kN/m<sup>2</sup>, 207 kN/m<sup>2</sup>,

276 kN/m<sup>2</sup>, and 414 kN/m<sup>2</sup>. During these drained tests, the axial stress was increased and the cell pressure was reduced so that the mean normal stress,  $p'$ , remained constant. The effective stress path for a constant  $p'$  drained test will lie in between the effective stress paths for an undrained test and a fully drained test with constant cell pressure. Thus, the volumetric strain experienced by these specimens would be less than those experienced by the specimens sheared under fully drained condition with constant cell pressure.

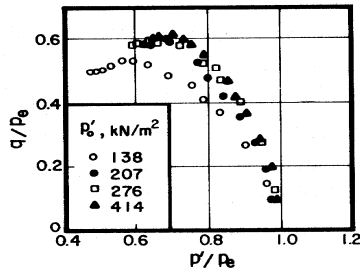


FIG. 14.—State Paths Followed during Constant  $p'$  Drained Tests

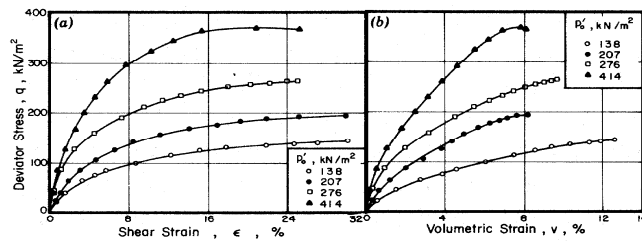


FIG. 15.—Constant  $p'$  Drained Tests: (a)  $q, \epsilon$  Relationship; (b)  $q, v$  Relationship

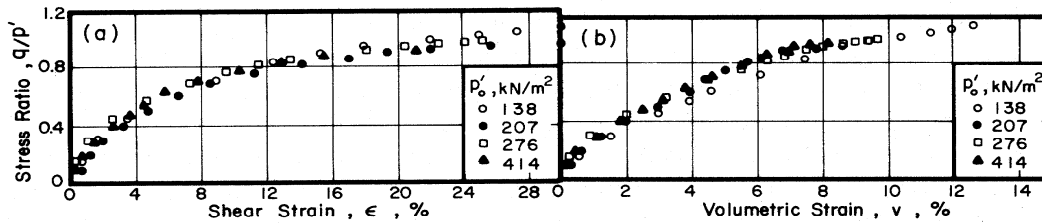


FIG. 16.—Constant  $p'$  Drained Tests: (a)  $q/p', \epsilon$  Relationship; (b)  $q/p', v$  Relationship

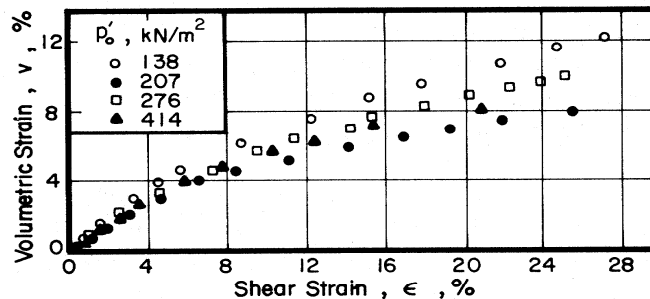


FIG. 17.— $v, \epsilon$  Relationship for Constant  $p'$  Drained Tests

**State Paths Followed during Constant  $p'$  Drained Tests.**—The state paths followed by the specimens sheared under constant  $p'$  drained conditions are shown in Fig. 14. Except for the specimen sheared from the lowest preshear consolidation pressure (138 kN/m<sup>2</sup>), for all other specimens the state paths are approximately the same. These state paths are examined in detail by the first writer, et al. (6).

**Stress-Strain Relationships.**—Figs. 15(a) and 15(b) show the  $q, \epsilon$  and  $q, v$



relationships for all the specimens sheared under constant mean normal stress conditions. The behavior exhibited by these specimens is similar to that exhibited by the fully drained test specimens sheared with constant cell pressure conditions.

In the case of undrained tests and fully drained tests with constant cell pressures, the stress ratio strain relationships were unique for each type of test. Similar unique relationships between the stress ratio and the strains are observed in Figs. 16(a) and 16(b) for the constant  $p'$  drained tests.

Finally, the  $(v, \epsilon)$  relationships for all the specimens sheared under constant  $p'$  drained conditions are presented in Fig. 17.

**Peak Stress Conditions.**—Figs. 18 and 19 contain the data corresponding to peak stress conditions in the  $q, p', w, \log p',$  and  $w, \log q$  plots. The slope of the critical state line in the  $q, p'$  plot is 0.93. The corresponding value of the angle of internal friction being  $23.7^\circ$ . The parameter,  $M$ , for constant  $p'$  drained tests is found to be close to that obtained from fully drained tests with constant cell pressures, but significantly different from the value for

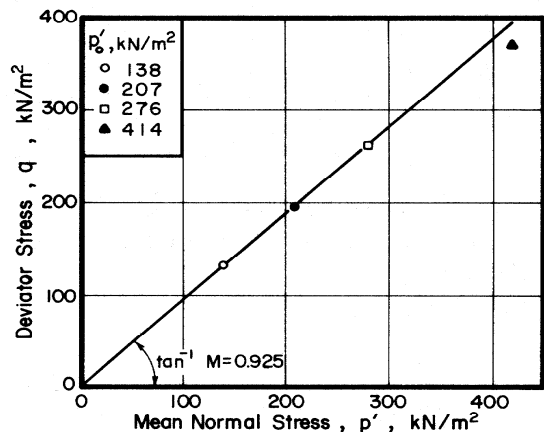


FIG. 18.—Peak Stress Points for Constant  $p'$  Drained Tests in  $q, p'$  Plot

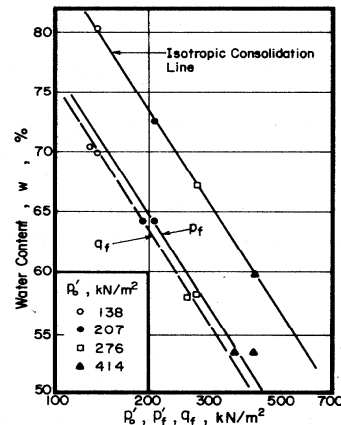


FIG. 19.—States of Samples in  $w, \log p'$  and  $w, \log q$  Plots

undrained tests. A similar observation was also noted for the behavior of Kaolin specimens by James and the first writer (8). These authors suggested that, for undrained conditions,  $p'_f/p'_o < 1$  and the peak stress envelopes for values of  $p'_f/p'_o < 1$  correspond to the Hvorslev failure Envelope. However, when  $p'_f/p'_o \geq 1$  (which include fully drained tests with constant cell pressure and constant  $p'$  drained tests), the peak stress envelope coincides with the critical state line. The  $w_f, \log p'_f$  and  $w_f, \log q_f$  relationships for constant  $p'$  drained tests are also found to be each parallel to the isotropic consolidation curve.

#### RESULTS OF ANISOTROPIC CONSOLIDATION TESTS

Altogether, five anisotropic consolidation tests were carried out in this series. These tests corresponded to stress ratios  $\eta$  of 0.0, 0.2, 0.4, 0.6, and 0.8. All specimens were isotropically consolidated to  $103.5 \text{ kN/m}^2$  and were then sheared under fully drained condition with constant cell pressure until the relevant stress ratio was reached. During anisotropic consolidation, the stress ratio,  $q/p'$ , was

maintained constant. The ratio of the principal effective stresses was, therefore, also constant. Thus

$$\eta = \frac{q}{p'} = 3 \frac{K-1}{K+1} \dots \dots \dots (7)$$

$$\text{in which } K = \frac{\sigma'_1}{\sigma'_3} \dots \dots \dots (8)$$

**Stress and State Paths during Anisotropic Consolidation.**—Fig. 20 shows the stress paths followed by the specimens during isotropic consolidation ( $\eta = 0$ )

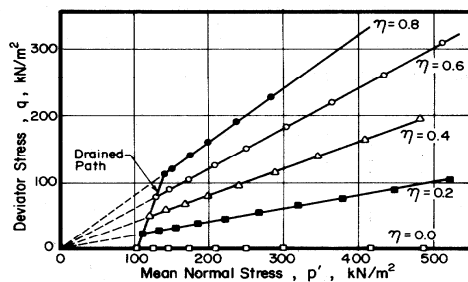


FIG. 20.—Stress Paths Followed during Isotropic and Anisotropic Consolidation

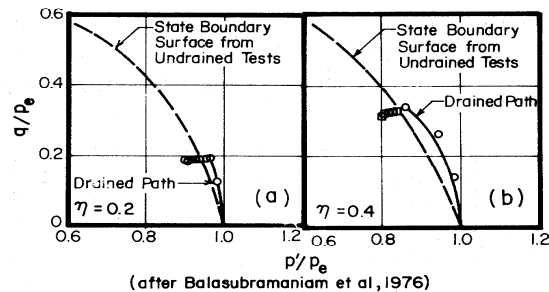


FIG. 21.—State Paths Followed by Two Specimens during Anisotropic Consolidation

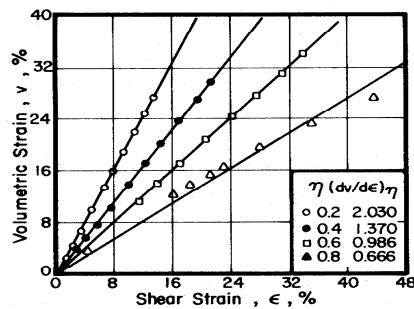


FIG. 22.—Strain Paths Followed during Anisotropic Consolidation

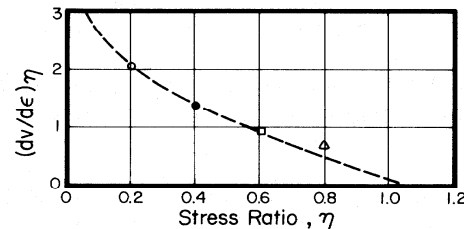


FIG. 23.—Variation of  $(dv/d\epsilon)_\eta$  with  $\eta$

and anisotropic consolidation. The corresponding state paths for two specimens are shown in Figs. 21(a) and 21(b). In these figures the dotted curve corresponds to the state boundary surface as obtained from undrained tests. Note that the state paths during anisotropic consolidation do lie close to the state path obtained from undrained tests. Ideally, the data for each anisotropic consolidation test should plot as a single point on the undrained state path.

**Strain Paths Followed during Anisotropic Consolidation.**—Fig. 22 shows the strain paths followed by each specimen during anisotropic consolidation. Note that the strain path in the  $v, \epsilon$  plot is linear for each anisotropic consolidation test. It is therefore apparent that the strain increment ratio  $(dv/d\epsilon)_\eta$  during

anisotropic consolidation is only a function of the stress ratio,  $\eta$ . Thus

$$\left( \frac{dv}{d\epsilon} \right)_{\eta} = f_2(\eta) \quad \dots \dots \dots (9)$$

The values of  $(dv/d\epsilon)_{\eta}$  observed for the four tests are 2.03, 1.37, 0.99, and 0.67. These values correspond to  $q/p'$  values of 0.2, 0.4, 0.6, and 0.8, respectively. Fig. 23 shows the variation of  $(dv/d\epsilon)_{\eta}$  with  $\eta$  and it is noted that the value of  $(dv/d\epsilon)_{\eta}$  close to the critical state is virtually zero.

**Variation of Void Ratio with Logarithm of Mean Normal Stress.**—The variation of the void ratio with the logarithm of mean normal stress is plotted in Figs.

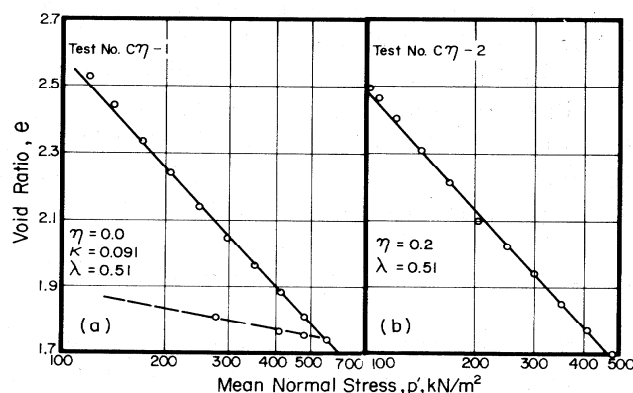


FIG. 24.— $e, \log p'$  Characteristics during Anisotropic Consolidation

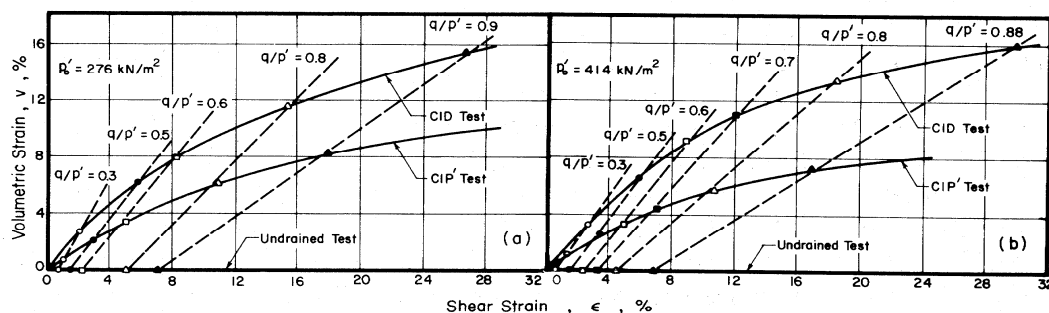


FIG. 25.—Constant Stress Ratio Contours Superposed on Strain Paths

24(a) and 24(b) for the two cases,  $\eta = 0$  and  $\eta = 0.2$ . For both cases, the void ratio is found to vary linearly with the logarithm of mean normal stress. Also, it is interesting to note that the slope of  $e, \log p'$  characteristics is approximately the same. The value of  $\lambda$  (the slope of isotropic and anisotropic consolidation line in  $e, \log p'$  plot) for  $\eta = 0.0, 0.2, 0.4, 0.6$ , and  $0.8$  are 0.51, 0.51, 0.515, 0.51, and 0.53, respectively. This observation is in good agreement with the theories developed at Cambridge and with the concept of normalized stress-strain behavior proposed by Ladd (9). Fig. 24(a) also contains the data from an isotropic swelling test. The slope,  $k$ , of the  $e, \log p'$  characteristics during isotropic swelling is found to be 0.07.

**BEHAVIOR OF SOFT BANGKOK CLAY IN STRESS RATIO STRAIN SPACE**

The first writer (5) has presented data on remolded specimens of Kaolin (sheared under a wide variety of applied stress paths) to illustrate that, provided the stress ratio,  $q/p'$ , increases, then for all specimens sheared from an isotropic stress state, a unique relation exists between the volumetric strain, shear strain, and the stress ratio. Also, specimens sheared in extension revealed a similar relationship to that of specimens sheared in compression. The first writer (5) plotted the strain paths for specimens sheared from an isotropic stress state along stress paths with increasing stress ratio. Contours of constant  $q/p'$  are found to be linear in this plot. Thus, the first writer (5) derived expressions for the volumetric and shear strains in terms of the stresses ( $q, p'$ ).

Figs. 25(a) and 25(b) show the strain paths followed by undrained, constant  $p'$  drained, and fully drained (with constant cell pressure) test specimens of soft Bangkok clay. The contours of constant  $q/p'$  are also superimposed in these figures. The contours are found to be straight lines in these plots. It appears, therefore, that  $q/p'$ ,  $v$ , and  $\epsilon$  are uniquely related for specimens that are sheared under stress paths with increasing  $q/p'$ .

**PREDICTION OF STRAINS USING INCREMENTAL STRESS-STRAIN THEORY**

An incremental stress-strain theory was proposed by Roscoe and Poorooshasb (14) for the prediction of strains in drained tests with different applied stress paths. In this theory, the volumetric strains in drained tests are determined using the unique state boundary surface obtained from undrained tests. Then, the shear strains in the drained tests are calculated using: (1) The stress-ratio shear strain relationship from undrained tests; (2) the slope of the anisotropic consolidation tests in ( $v, \epsilon$ ) space; and (3) the volumetric strains computed for the drained tests, using the state boundary surface from undrained tests. The value of  $\lambda$  used in the prediction of volumetric strain is 0.51 and is obtained from the isotropic and anisotropic consolidation tests.

The procedure for calculating the volumetric strain and the shear strain is described in detail by the first writer (4). The predicted strains and the experimentally observed strains are presented in Figs. 26(a)–26(c) and Figs. 27(a) and 27(b) for fully drained tests with constant cell pressure and for constant  $p'$  drained tests. The experimental points are shown by circles and the predictions from the theory by dashed lines. The incremental stress-strain theory of Roscoe and Poorooshasb is found to predict very closely the experimentally observed strains.

**PREDICTION OF STRAINS USING CRITICAL STATE THEORIES**

In this section, the experimentally observed strains are compared with the strains predicted from the critical state theories. Two theories are employed and these are the Cam Clay Theory, by Roscoe, Schofield, and Thurairajah (15) and Schofield and Wroth (17); and the Revised Theory by Roscoe and Burland (13).

The fundamental soil parameters used in the Critical State Theories and  $\lambda$ ,  $k$ , and  $M$ , in which  $\lambda$  = the slope of the isotropic consolidation line in the

$e, \log p'$  plot;  $k$  = the slope of the isotropic swelling line in the  $e, \log p'$  plot; and  $M$  = the slope of the critical state line in the  $q, p'$  plot. Isotropic consolidation and swelling tests carried out on soft Bangkok clay indicate that the value of  $\lambda$  is 0.51 and that of  $k$  is 0.091. Also, the critical state parameter,  $M$ , is taken as 1.0.

In the Revised Theory of Roscoe and Burland, corrections are made for the shear strain from the contribution due to the constant  $q$  yield loci. The contributions from the constant  $q$  yield loci were approximately the same as the shear strain obtained from undrained tests in the  $q/p', \epsilon$  plot.

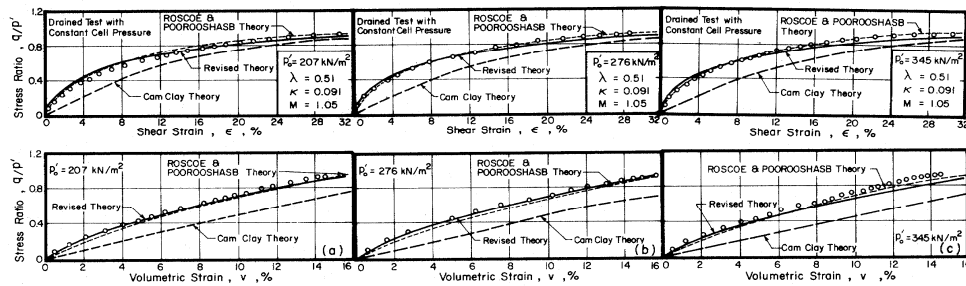


FIG. 26.—Experimentally Observed Strains Compared with Predictions from Incremental Stress-Path Theory

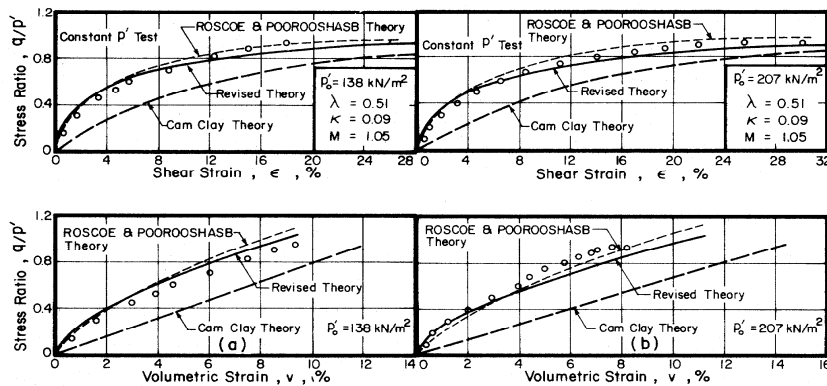


FIG. 27.—Experimentally Observed Strains Compared with Predictions from Critical State Theories

The predicted strains for five of the tests are shown in Figs. 26(a)–26(c) and 27(a) and 27(b). From these figures, the following conclusions are reached: (1) The Cam Clay Theory overpredicts the volumetric strain and the shear strain; and (2) the Revised Theory successfully predicts the strains in all tests.

## CONCLUSIONS

A comprehensive series of triaxial compression tests were carried out on soft Nong Ngoo Hao clay and the results obtained were compared with the theoretical prediction. Four types of triaxial tests were carried out and these

included undrained tests, constant mean normal stress drained tests, fully drained tests with constant cell pressure, and anisotropic consolidation tests. The following conclusions are reached:

1. For all types of tests, the state paths followed by the specimens are found to be nearly the same (especially at low levels of deviator stresses where settlement computations are often carried out) though slight deviations are noted with increase in preshear consolidation pressure.
2. For each type of test, the stress ratio strain relationships are also found to be nearly coincident and independent of the preshear consolidation pressure.
3. For all specimens sheared from an isotropic stress with increasing stress ratio, a unique relationship is found between the stress ratio,  $q/p'$ , and the strains,  $v$  and  $\epsilon$ .
4. During anisotropic consolidation, the voids ratio is found to vary linearly with the logarithm of the mean normal stress and the strain increment ratio,  $(dv/d\epsilon)_\eta$ , is a constant for any particular stress ratio,  $\eta$ .
5. For each type of shear test in which the specimens were taken to failure, the end points are found to lie on straight lines in  $q$ ,  $p'$ ,  $w$ ,  $\log p'$ , and  $w$ ,  $\log q$  plots. The parameter,  $M$ , and the angle of internal friction,  $\bar{\phi}$ , are found to be nearly the same for constant  $p'$  and fully drained tests. The  $\bar{\phi}$  value obtained from constant  $p'$  drained tests is  $21.7^\circ$  and the corresponding value from fully drained tests with constant cell pressure is  $23.7^\circ$ . These values deviated from the corresponding value ( $\bar{\phi} = 26^\circ$ ) obtained from undrained tests.
6. The incremental stress-strain theory of Roscoe and Poorooshasb (14) is found to predict the strains in constant  $p'$  drained tests and in fully drained tests with constant cell pressures.
7. The Cam Clay Theory overpredicted the strains in all tests and the Revised Theory of Roscoe and Burland (13) successfully predicted the strains in all tests.

#### ACKNOWLEDGMENTS

The work presented in this paper was carried out at the Asian Institute of Technology. Thanks are due to Ruangvit Chotivitayathanin and Suvit Viranuvut for their assistance in carrying out the experimental program. Thanks are also due to Za-Chieh Moh, Edward W. Brand, Vatinee Chern, and Uraiwan Singchinsuk.

#### APPENDIX.—REFERENCES

1. Balasubramaniam, A. S., "Some Factors Influencing the Stress-Strain Behaviour of Clays," thesis presented to Cambridge University, at Cambridge, England, in 1969, in partial fulfillment of the requirements for the degree of Doctor of Philosophy.
2. Balasubramaniam, A. S., "Stress History Effects on Stress-Strain Behaviour of a Saturated Clay," *Geotechnical Engineering, Journal of Southeast Asian Society of Soil Engineering*, Vol. IV, No. 2, 1973, pp. 91-111.
3. Balasubramaniam, A. S., "A Critical Study of the Uniqueness of State Boundary Surface for Saturated Specimens of Kaolin," *Geotechnical Engineering, Journal of Southeast Asian Society of Soil Engineering*, Vol. V, No. 1, 1974, pp. 21-38.
4. Balasubramaniam, A. S., "A Critical Re-appraisal of the Incremental Stress-Strain Theory for Normally Consolidated Clays," *Geotechnical Engineering, Journal of*

- Southeast Asian Society of Soil Engineering*, Vol. VI, 1975, pp. 15–32.
5. Balasubramaniam, A. S., "Behaviour of a Normally Consolidated Clay in Stress Ratio Strain Space," *Symposium on Recent Developments in the Analysis of Soil Behaviour and their Application to Geotechnical Structures*, University of New South Wales, Sydney, Australia, 1975, pp. 275–287.
  6. Balasubramaniam, A. S., et al., "State Boundary Surface for Weathered and Soft Bangkok Clay," *Australian Geomechanics Journal*, Vol. 6, 1976, pp. 43–50.
  7. Henkel, D. J., "Relationship between Effective Stresses and Water Content in Saturated Clays," *Geotechnique*, London, England, Vol. 10, No. 2, 1960, pp. 41–54.
  8. James, R. G., and Balasubramaniam, A. S., "The Peak Stress Envelopes and Their Relations to the Critical State Line for a Saturated Clay," *Proceedings of the 4th Asian Regional Conference on Soil Mechanics and Foundation*, Bangkok, Thailand, 1971, pp. 115–120.
  9. Ladd, C. C., "Stress-Strain Behaviour of Saturated Clay and Basic Strength Principles," *Research Report R64-17*, Massachusetts Institute of Technology, Cambridge, Mass., 1964.
  10. Lambe, T. W., "Methods of Estimating Settlement," *Journal of the Soil Mechanics and Foundations Division*, ASCE, Vol. 90, No. SM5, Proc. Paper 4060, Sept., 1964, pp. 43–67.
  11. Mitchell, R. J., "Some Aspects of the Critical State Theories of Yielding of Soils," thesis presented to Cambridge University, at Cambridge, England, in 1967, in partial fulfillment of the requirements for the degree of Doctor of Philosophy.
  12. Rendulic, L., "Relation Between Voids Ratio and Effective Principal Stresses for a Remoulded Silty Clay," *Proceedings of the 1st International Conference on Soil Mechanics and Foundation Engineering*, Cambridge, Mass., Vol. 3, 1936, pp. 48–51.
  13. Roscoe, K. H., and Burland, J. B., "On the Generalised Stress-Strain Behaviour of Wet Clay," *Engineering Plasticity*, Cambridge University Press, Cambridge, England, 1968, pp. 535–609.
  14. Roscoe, K. H., and Poorooshasb, H. B., "A Theoretical and Experimental Study of Strains in Triaxial Tests on Normally Consolidated Clays," *Geotechnique*, London, England, Vol. 13, 1963, pp. 12–38.
  15. Roscoe, K. H., Schofield, A. N., and Thurairajah, A., "Yielding of Clays in States Wetter than Critical," *Geotechnique*, London, England, Vol. 13, 1963, pp. 211–240.
  16. Roscoe, K. H., Schofield, A. N., and Wroth, C. P., "On the Yielding of Soils," *Geotechnique*, London, England, Vol. 8, 1958, pp. 22–53.
  17. Schofield, A. N., and Wroth, C. P., *Critical State Soil Mechanics*, McGraw-Hill Book Co. Ltd., London, England, 1968.
  18. Skempton, A. W., "The Pore Pressure Coefficients *A* and *B*," *Geotechnique*, London, England, Vol. 4, 1954, pp. 143–147.
  19. Walker, L. K., "The Deformation of Clay as a Time Dependent Process," thesis presented to Cambridge University, at Cambridge, England, in 1967, in partial fulfillment of the requirements for the degree of Doctor of Philosophy.
  20. Wroth, C. P., "The Prediction of Shear Strain in Triaxial Tests on Normally Consolidated Clays," *Proceedings of the 6th International Conference on Soil Mechanics and Foundation Engineering*, Montreal, Canada, Vol. 1, 1965, pp. 417–442.

---

## 14040 DEFORMATION, STRENGTH OF SOFT BANGKOK CLAY

**KEY WORDS:** Clays; Consolidation; Deformation; Shear strength; Thailand; Triaxial tests

**ABSTRACT:** A comprehensive series of stress controlled triaxial compression tests was carried out on Soft Bangkok Clay. Undisturbed samples of soft clay were taken from Nong Ngoo Hao, a site situated about 15 km east of the coast in the Chao Phraya Plain. Altogether, four different types of triaxial tests were carried out and these include: (1) Undrained tests with constant cell pressure and with 1-hr and 1-day load increment durations; (2) fully drained tests with constant cell pressure; (3) constant mean normal stress tests under drained conditions; and (4) anisotropic consolidation tests. The experimentally observed stress-strain behavior is compared with the predictions from various stress-strain theories.

**REFERENCE:** Balasubramaniam, A. S., and Chaudry, A. R., "Deformation and Strength Characteristics of Soft Bangkok Clay," *Journal of the Geotechnical Engineering Division*, ASCE, Vol. 104, No. GT9, **Proc. Paper 14040**, September, 1978, pp. 1153-1167